A rapid groundwater circulation system inferred from temporal water dynamics and isotopes in a typical alluvial-fluvial fan of the Nalenggele River in arid Qaidam Basin, China

Hongbing Tan*[1)], Yu Zhang[1)], Wenbo Rao*[1)], Wanquan Ta[2)], Hongye Guo[2)], Shicheng Lu[1)], Peixing Cong[1)]

1) School of Earth Sciences and Engineering, Hohai University, Nanjing, China;

2) Qinghai Province Hydrogeology and Engineering Geology Environmental Institute of Geological Survey, Xining, China;

3) Cold and Arid Regions Environmental and Engineering Research Institute, Chinese Academy of Sciences, Nanzhou, China

* Corresponding author: Hongbing Tan (tan815@sina.com); Wenbo Rao (raowenbo@163.com)

Key Points:

- A rapid groundwater circulation system has been approved.
- Water source, macro-structures and large hydraulic head governing rapid circulation.
- Warming climate is expected to increase recharge groundwater.

Abstract

A rapid groundwater recharge and circulation system has developed in Qaidam Basin, China. Stable H and O isotopes were monthly sampled in both river water and groundwater, and water table fluctuations were monitored over a complete seasonal cycle from dry-season to wet-season conditions in the Nalenggele River catchment in Qaidam Basin. The main goals are to demonstrate and explain rapid circulation in the groundwater system. A distinct seasonal fluctuation of the water table with associated stable isotopic variations can be observed in the alluvial-fluvial fan of the Nalenggele River catchment. During the wet season, replenishment of the aquifer results in a rising water table rises. The recharge mechanism appears to be related to the coincidence of several favorable hydrological conditions: an abundant recharge water source from summer precipitation and glacial-snow melt in the high Kunlun mountains, large-scale active faults, a volcanic crater and other macro-structures that act as favorable recharge conduits, the large hydraulic head from recharge areas to the alluvial-fluvial fan, and the presence of over 100 m of unconsolidated sand and gravel acting as the main aquifer. Warming climate is expected to increase precipitation and to accelerate melting of glaciers in the Kunlun Mountains, increasing recharge and leading to rapid rise in the water table in the alluvial-fluvial fan. Increased recharge in the future will provide water of improved quality to the Qaidam Basin, and will allow management of land in ways that reduce soil salinity and alkalinity.

1 Introduction

Many studies conclude that groundwater should be very old in arid or semi-arid basins, e.g. most basins or plateaus in northern China and deserts（Ma et al., 2009; Jiang et al., 2019）. Globally, there is a growing body of evidence suggesting that many of Earth's aquifers contain 'fossil' groundwater that was recharged more than 12,000 years ago, and only a very small portion of groundwater was recharged in the last 50 years (Gleeson et al., 2016; Jasechko et al., 2017; Smerdon et al., 2017). However, in most basins, rainwater also finds its way through macropores and preferential pathways to shallow unconfined aquifers within hours of falling (Glenn et al., 2015; Hartmut et al., 2019). At present, the nature of rapid groundwater circulation or even seasonal recharge in arid basins that are remote from recharge sources remains unclear. The mechanisms or conceptual models governing the rapid recharge need to be further investigated. In addition, the global volume and distribution of groundwater less than 50 years old, which is the most vulnerable

to global climate change, are unknown (Gleeson et al., 2016). Given the expected challenges arising from future global and regional climate changes, it is important to improve the understanding of aquifers dominated by young groundwater. Accurate assessment of water resources and clear understanding of the hydrology in such aquifers will be important to future management of groundwater use, of ecological changes in vulnerable environments, and of secondary hazards resulting from rising groundwater levels.

The Nalenggele River (NR) catchment was selected as the study area. It is a typical large river draining the high and cold area of the northern slope of the eastern Kunlun Mountains (KM) and ending in the western Qaidam Basin (QB) (Fig. 1). In this region, sources of groundwater recharge, spatial and temporal variations of runoff and interactions between groundwater and stream flow are very complex and remain unclear. There have been a few previous studies on a surface-groundwater system in the NR catchment and adjacent area in the Golmud and Nomhon River catchments (Xiao et al. 2017a and b; Xu et al., 2017). These previous studies found that the groundwater systems resembled a typical mountain-basin system. However, it remains unclear why water tables at depths of 10 to 50m or even deeper fluctuate so greatly under natural conditions. Such changes are difficult to explain with an ancient recharge model. In the absence of monthly monitoring data, it is not known whether seasonal changes in water table depth are associated with changes in stable H and O isotopes in groundwater. The previous conclusions were mainly dependent on ^{14}C to determine the age of groundwater. However, neither methods are capable of resolving differences among seasonal pulses of recharge. It is of critical importance to confirm rapid (annual, seasonal or even daily) recharge of groundwater in an arid basin. This will directly relate to accurate assessment of groundwater resources and their management. Thus, a systematic and detailed study is necessary for groundwater systems like those in the extremely arid QB, particularly in the alluvial-fluvial fan (AFF) of the NR catchment where groundwater appears to be abundant.

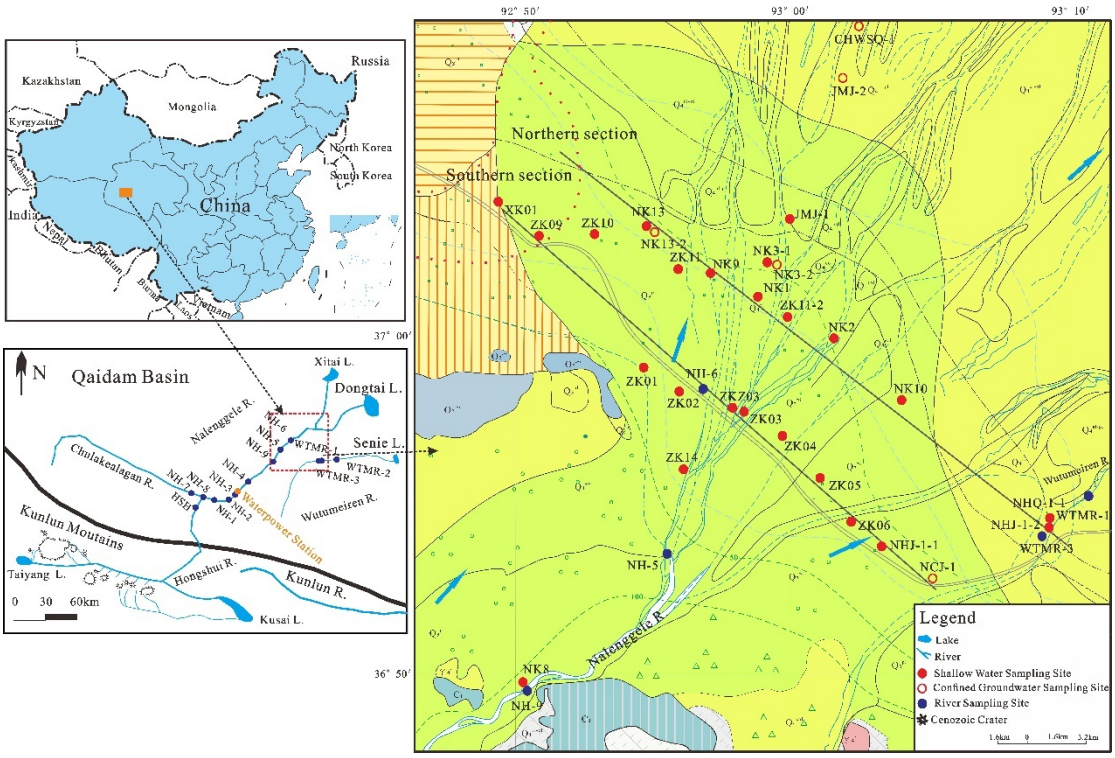

Figure 1 Simplified hydrogeologic map of the Nalenggele River catchment and location of the sampling sites (Two monitoring sections: southern and northern sections are located around the centre and near the northern edge of an alluvial-fluvial fan).

In recent years, the prospect of warming arising from climate change has led to concerns over large-scale shrinkage of glaciers and subsurface permafrost degradation in the source regions of rivers in the Tibetan Plateau (Cheng and Wu, 2007; Yang et al., 2007; Ge et al., 2008; Zhang et al., 2013). Therefore, Tibet has become a focus of global interest as hydrologists assess the variation of surface runoff and recharge in the main river catchments with the aim of predicting future changes. Recent observations show significant warming on the Tibetan Plateau during the past several decades (Chen et al., 2013; Gao et al., 2015; You et al., 2015), and climate models predict warming will continue in the future (Rangwala et al., 2010; Ji and Kang, 2013; Zhu et al., 2013; Sun et al., 2015). Recent reports state that the glacial area has declined by 15% and the permafrost area has decreased by 16%, whereas the lake area has increased from 40000 km^2 to 47400 km^2 over the past 50 years in the Tibetan Plateau (Li et al., 2020). Satellite gravity data together with multiple hydrologic models provide clear evidence of increasing groundwater storage in the eastern Tibetan Plateau, again reflecting increased abundance of glacial meltwater (Xiang et al., 2016). In particular, the GRACE data analysis discovered that the variation of total water storage (TWS) showed a

distinct upward trend in QB (Jiao et al., 2015; Wang et al., 2018). Correspondingly, the most significant climate warming is found in the QB (Chen et al., 2013; Wang et al., 2014; Kuang et al., 2016). From 1961 to 2010, the annual mean temperature in the QB increased by 0.53°C decade^{-1} and the annual mean temperature increased about 2.65°C (Wang et al., 2014). Without doubt, such warming will lead to significant changes in hydrology and water resources on the Tibetan Plateau, particularly in arid QB.

Research interest in the response of glaciers to global warming is not confined to the Tibetan Plateau. The topic is being addressed in other regions (e.g. Mark, 2003; Bijeesh et al., 2017), but is in its infancy, and many aspects remain to be studied (Aude et al., 2019). In alpine cold-arid basins, the prevalent viewpoint is that massive recharge happened as a result of melting of ice just after the Last Glacial Maximum (LGM) (Post et al., 2013; Salamon, 2016). Some studies concluded that the depleted isotopic signatures of groundwater in North China Plain indicate recharge of palaeo-waters during glacial–interglacial transitional periods (Chen et al., 2003; Currell et al., 2010; Gates et al., 2008). However, it remains to be confirmed whether global recharge after the LGM indeed occurred. Glacier meltwater has commonly been suggested as a substantial source of recharge for nearby porous, karstic, or fractured-rock aquifers. Malard et al. (2016) identified a karstic aquifer under the Fonds glacier (Swiss-French border) and determined that for karst in Swiss alpine areas above 2500 m, recharge is due both to precipitation and to glacier melting. Another mode of rapid groundwater recharge may occur in fractured-rock aquifers or faults acting as conduits, but is less frequently observed. Chen and Wang (2009) concluded that the 2003 M6.1 earthquake in the Hexi Corridor in China caused local groundwater to be greatly increased recharge from the Qilian Mountains through numerous seismically-active faults that crisscross the Corridor. In summary, traditional hydrological theories proposed that groundwater recharge is a very slow process in arid basins, occurring far away from water sources, and did not allow for dominantly young groundwater with distinct pulses of annual or seasonal recharge in arid basins. This may indeed apply in arid basins with almost no recharge from local precipitation, but has not been demonstrated in all cases, in particular for arid basins adjacent to high-cold mountains.

Isotopes of hydrogen and oxygen have been widely used in hydrologic studies of water circulation processes (Clark et al.1997; Kendall et al., 1998; Tian et al., 2007; Pradeep et al., 2010). The radioisotope ^{222}Rn has also been used to identify groundwater discharge to rivers (Smerdon et al. 2012; Yael et al., 2015; Su et al. 2015; Xu et al., 2017). Transient activities of radon isotopes are

usually high in groundwater that has been in contact with rock bearing parent nuclides (Krishnaswami et al., 1982). High Rn concentrations are focused near points of discharge from fractures in certain granitoids (Gascoyne et al., 1993). Thus, ^{222}Rn can be used to identify buried faults acting as conduits for groundwater. In addition, helium isotope ratios ($^{3}He/^{4}He$) are excellent natural tracers for locating deep faults and tracing groundwater circulation along deep faults in the Earth's crust (Gascoyne et al., 1993; Kennedy et al., 1985; Weiss, 1971; Tolstinkhin et al., 1996; Kennedy and Matthijs, 2006).

In this study, stable H and O isotopes were monitored in river water and AFF groundwater of the NR catchment at monthly intervals over a complete seasonal cycle from dry-season to wet-season conditions. Tritium and ^{222}Rn were also measured for water under base conditions in the dry season in April. In addition, several years' observations of water table fluctuation at monthly time-scale are discussed. The study focused on the following goals: 1) determining relationships between spatial and temporal fluctuation of water tables and stable isotopic variations over a complete seasonal cycle from dry-season to wet-season conditions; 2) demonstrating rapid circulation in the groundwater system and determining the recharge mechanism; and 3) predicting the effects of future climate warming on water table fluctuations and groundwater storage.

2 Study area and methods

2.1 Hydrology and geography

The lower reach of the NR catchment is located in the southwest part of QB and is managed by Golmud city in Qinghai province, China (Fig. 1). The climate is a typical inland dry climate with very scarce precipitation, strong wind and intense evaporation. The winter is very long but the summer is short with a large diurnal temperature variation. According to data from Xiaozaohuo meteorological station, precipitation occurs mainly between late May and September, and averages 29.8mm annually. The annual average potential evaporation is nearly 100 times the total precipitation. The average annual temperature ranges from 2.6 to 4.3 °C and the highest monthly average temperature (ranging from 15.1 to 18.7°C) generally occurs in July. No meteorological records exist for the high mountainous parts of the NR catchment because of the harsh natural conditions, but the glaciers and snow are widespread, and precipitation, also dominantly in summer, should be much higher than in the lower parts of the basin. Large storms and floods frequently occur in summer in the mountains. The mountains are uninhabited, and the lower reach of the basin

is sparsely inhabited, so that the eco-environment remains in a nearly natural state. However, a large water control project to be built in the coming 10 years in the middle reach of NR will most likely affect natural hydrology, hydrogeology and water resources in the lower reach.

The NR, which rises in the eastern KM, is the largest river in QB with a length of over 435km and a catchment area of about 21898km^2. No flow gauges are installed on the river, so that systematic hydrometric data are unavailable. An estimate of the total annual runoff is about 10^9 m^3/a (Wang et al., 2008). Field observations in 2019 (this study) indicated that the river runoff in the mountains shows a large seasonal change. In winter, base flow is maintained by mountain spring discharge. In spring and early summer, flow is supplied by melt water from snow and glaciers. Both melt water and runoff from summer precipitation contribute to flow during the humid season, June to September. In particular, frequent heavy rainstorms strongly affect summer runoff in August and September. According to field estimates, the base flow in April seems to be similar in volume in the two largest tributaries, the Hongshui River (HR) and Chulakealagan River (CR) in the upper catchment. However, the runoff in the HR is distinctly larger than that in the CR in July. The mainstream is generally dry at the driest time of the year from November to April. At other times, river water discharges into the basin, but even in summer season when flow is greatest, over 70% of surface water infiltrates before reaching the basin (Wang et al., 2008). In the wet season, groundwater discharged from springs at the downgradient limit of the AFF converges into streams that flow north into the QB, terminating in salt lakes (Fig. 1).

2.2 Basic hydrogeology of groundwater system

The upper catchment of the NR is located in the northern slope of eastern KM at elevations from 2,800 to over 5,000 m above sea level (a.s.l.). Intense neotectonic activity is expressed as a set of high-angle thrust faults parallel to the range front, a secondary set of tensile faults approximately perpendicular to the thrust faults, and a set of volcanic vents. Some faults extend to lower parts of the basin (Fig. 2). Part of the melt water and precipitation inform the high elevations converges into surface water in streams and mountain lakes. Some surface water infiltrates through faults, fissures and volcanic edifices to a fractured-rock aquifer in the mountains. The groundwater developed in the high mountains flows towards the basin, locally discharge into rivers where favorable geological and geomorphological conditions exist. The river and the fractured-rock aquifer are closely connected, and exchange water over the entire hard-rock stream bed. According to aquifer types, physical properties and water dynamics, four kinds of aquifer are present:

fractured bedrock, karst, consolidated clastic sedimentary rock with intergranular porosity in addition to fracture porosity, and unconsolidated sediment. A fifth occurrence takes the form of ice in frozen soil and rock at high latitudes. Since the Quaternary period, the western QB in front of eastern KM has been subsiding, resulting in the deposition of thick, unconsolidated sediment sequences in the basin. These deposits from a set of large, porous aquifers with great water-yield potential. The maximum thickness of the phreatic aquifer in the mountain region is probably tens of meters, while the total thickness of the phreatic aquifer and multiple confined aquifers in the alluvial-fluvial fan and alluvial-fluvial plain is hundreds of meters. The confined groundwater may well up locally to replenish the upper phreatic aquifers or discharge direct to the surface as artesian flow through deep buried faults or "sky windows". The water table lies about 50 m below the surface at the mountain front, over 10 m in the center of the AFF, and intersects the surface at the foreland of the AFF mountains (Table 1). The aquifer system is over 100-200 m thick at the center of the fan. The AFF of the NR is the largest fan in the QB, and contains one of the richest groundwater resources in the area. The groundwater quality is excellent in all aquifers of the AFF and is almost undisturbed by development at present.

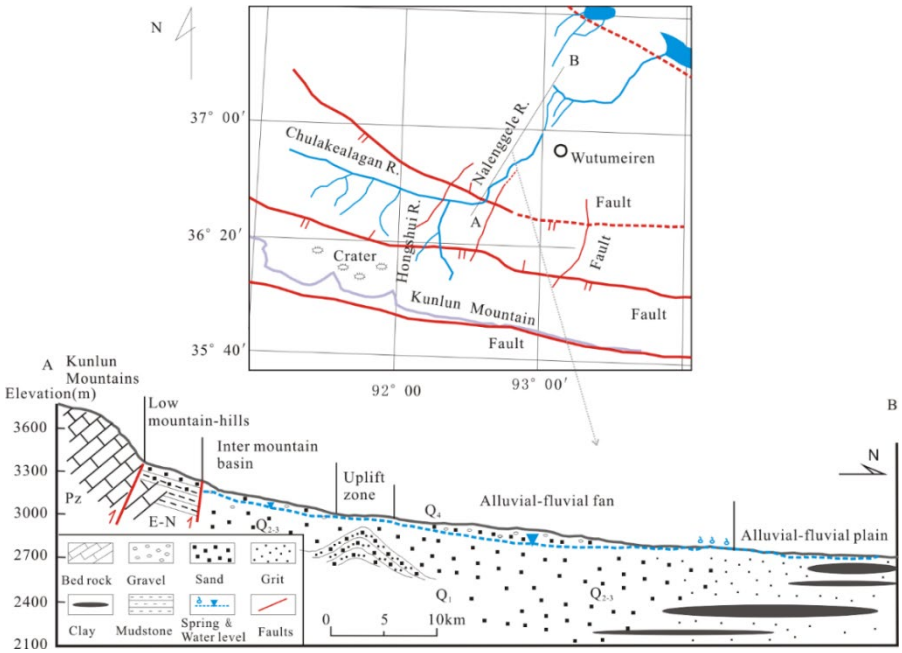

Figure 2 Simplified tectonic map of the source and upper reaches in the Nalenggele River and basic hydrogeologic section (A-A line)

222

Table 1 Basic information of sampling sites (well or spring)

Site	Sample number	Elevation /m	Well Depth/m	Type	Water yield/m^3/d	Water table/m	Aquifer thickness /m	Main lithology
Mountain	SDJ-1	3266		CW				Sands, gravel
Southern Section	XK01	2902		PW		22.86		Sands, gravel
	ZK10	2904	121.15	PW	5279	34.56	86.59	Sands, gravel
	ZK09	2905	120.10	PW	4761	33.93	86.17	Sands, gravel
	ZK01*	2940	150.3	PW	5495	32.23	107.23	Sands, gravel
	ZK02	2878	151.5	PW	8199	15.97	125.91	Sands, gravel
	ZK14	2974	150.60	PW	6307	19.29	120.37	Sands, gravel
	ZKZ03	2929	150.0	PW		27.15		Sands, gravel
	ZK03*	2924	150.0	PW	9685	26.97	119	Sands, gravel
	ZK04	2927	150.60	PW	8934	24.08	121.77	Sands, gravel
	ZK05*	2941	150.28	PW	9832	26.84	123.44	Sands, gravel
	ZK06*	2945	150.20	PW	9331	26.655	118.65	Sands, gravel
	NK8	3073	31.40	PW	1900	3.34	15.10	Sands, gravel
	NHJ-1-1	2925	70	CW		5.0		Sands, gravel
	NCJ-1	2909		CW		5.0		Sands, gravel
Northern Section	NK13	2876	250.2	PW	3675	8.06	212.7	Sands, gravel
	ZK11	2876	120.00	PW	8588	8.48	108.6	Sands, gravel
	NK9	2880	200.75	PW	2400	6.53	188.76	Sands, gravel, mud
	NK1	2879	251.00	PW	4259	7.79	222.28	Sands, gravel
	JMJ-1	2871	10	CG		0		Sands, grit
	JMJ-2	2826	10	CG		0		Sands, grit
	CHWSQ-1	2823		Spring		0		Sands, grit
	NK3-1* NK3-2	2877	251 300	PW CG		1.19 0.35	92.29 170.35	Sands, gravel, mud
	ZK11-2	2885		PW		8.57		Sands, gravel
	NK2	2884	198.00	PW	1252	3.94	194.18	Sands, grit, mud
	NK10*	2886	250.63	PW	4242	0.45	92.55	Sands, gravel
	NHQ-1-1	2860		Spring		0		Sands, gravel
	NHJ-1-2	2858	15	CW		3.0		Sands, gravel

*Automatic gauge was installed to record groundwater table. CW-Civil well; PW-Phreatic groundwater; CG-Confined groundwater. Blank space means no data available.

223

224

225

226

227

228

2.3 Sampling strategy and measurements

Groundwater and river water samples were collected from early April to October (April, June, July, September and October) in 2019. Tritium, He isotopes and ^{222}Rn measurements of groundwater were made only on samples collected in April, which can represent the sample under the base condition. The monthly river samples were collected simultaneously (same period with groundwater sample) at sites from the high mountain zone to the northern edge of the AFF. Two monitoring sections for groundwater sampling and water table measurement are roughly perpendicular to the river channel around the AFF. The southern monitoring section cut through the center of the fan and included some wells near the mountain front. The northern monitoring section was located near the northern edge of the fan and included some shallow wells and springs near the edge of the fan (Fig. 1). Before sampling, the depth to the water table was measured first (some wells had automatic water-level meters installed). Given the typical well depths (150-250m) and depths to the water table (>10m), it was impractical to pump the wells dry before sampling. Instead, a special instrument (depth-setting sampler) was inserted at least 50 m below the water table to take the groundwater samples. The tritium, radon and inert gas samples were collected from water extracted by a bore-hole turbine pump driven by a high-power electromotor, after pumping for two hours in order to avoid atmospheric contamination to the greatest extent possible

Samples for stable isotopic analysis were sealed tightly in special thick plastic bottles. At the time of sampling, the electrical conductivity, pH, and temperature were measured using standard hand-held calibrated field meters. Because of its short half-life, ^{222}Rn was analyzed in the field using a DURRIDGE USA (RAD 7) radon detector. Five measurements were taken over 1 to 2 hours; the first was discarded, and the remaining four were averaged to yield the reported measurement. The detection limit was 0.4000 cpm/pCi/L. Data were accepted if the uncertainty of measurements fell within ±25% of the mean (confidence level: 95 percent). The measurement time was extended if the range of the readings exceeded ± 25%.

Measurements of stable H and O isotopes were performed at the State Key Laboratory of Hydrology-Water Resources and Hydraulic Engineering, Hohai University, Nanjing. The $^{2}H/^{1}H$ and $^{18}O/^{16}O$ ratios were measured on a MAT253 mass spectrometer, and the results are reported relative to VSMOW with analytical precisions (1σ) of ±1‰ to 2‰ and ±0.2‰ to 0.3‰, respectively. For the determination of the tritium content in groundwater, the water samples were concentrated through electrolysis and then measured by a low-background liquid scintillation counting (Tri-Carb

3170 TR/SL), and the results were expressed as absolute concentrations in tritium units (TU) with a precision (1σ) of ±0.8 TU or better, and a detection limit of 0.2 TU. Analytical techniques and instrumentation for He isotope analyses were similar to those described by Ye et al. (2007). He isotopes were measured using a MM5400 mass spectrometer in the Laboratory of Gas Geochemistry (Lanzhou), Institute of Geology and Geophysics, Chinese Academy of Sciences. $^{3}He/^{4}He$ ratios were reproducible in duplicate analyses to ±1%. All the results are listed in Table 2-3.

Table 2 Stable H and O and radio tritium isotopic data of groundwater samples in different months

Site	Sam. No.	April			June		July		September		Octobet		December		Std	
		δD‰	$\delta^{18}O$‰	T（TU）	δD‰	$\delta^{18}O$‰	δD‰	$\delta^{18}O$‰	δD‰	$\delta^{18}O$‰	δD‰	$\delta^{18}O$‰	δD‰	$\delta^{18}O$‰	δD	$\delta^{18}O$
Southern Section	XK01			8.22			-68.3	-9.37	-69.9	-10.31	-69.8	-10.09			0.7	0.40
	ZK10	-58.2	-9.22	19.07	-56.3	-8.24	-55.5	-7.93	-57.8	-9.42	-52.9	-6.98	-58.0	-9.54	1.9	0.92
	ZK09	-60.7	-9.14	8.25	-59.8	-9.16	-56.1	-7.61	-60.1	-9.41	-59.3	-9.09	-59.7	-9.26	1.5	0.60
	ZK01	-58.2	-9.31	15.44	-59.6	-9.19	-51.2	-6.27	-58.6	-9.50	-51.4	-6.95	-60.0	-9.93	3.7	1.39
	ZK02	-57.6	-9.21	13.39	-57.3	-7.94	-58.2	-9.16	-58.7	-9.36	-53.4	-7.87	-58.4	-8.95	1.8	0.61
	ZK14	-59.6	-9.40	10.33	-57.2	-8.88	-57.6	-9.45	-57.4	-9.41	-56.4	-9.32			1.0	0.21
	ZKZ03	-54.1	-8.60	9.20	-54.0	-8.50	-56.0	-8.85			-46.3	-5.94	-53.8	-8.17	3.4	1.06
	ZK03	-59.7	-9.31	8.71	-56.8	-7.96	-55.3	-8.34	-54.5	-8.80			-57.2	-8.96	1.8	0.47
	ZK04	-59.3	-9.36	8.14	-58.2	-9.04	-52.0	-7.21			-56.8	-7.77	-61.9	-9.63	3.3	0.95
	ZK05	-55.7	-8.41	8.56	-54.9	-7.94	-59.6	-9.00			-57.8	-8.91			1.8	0.43
	ZK06	-58.4	-9.12	8.22	-57.9	-8.47	-60.1	-8.82	-59.2	-9.18	-58.8	-9.13	-58.9	-9.65	0.7	0.36
	NK8			16.25			-50.2	-6.89					-56.1	-9.30	2.9	1.21
	NHJ-1-1	-54.9	-8.65	8.08			-56.0	-8.88							0.5	0.11
	NCJ-1	-55.2	-8.63	8.42			-49.6	-6.51							2.8	1.06
Nothern Section	NK13	-60.2	-9.14	7.85	-59.6	-9.16	-59.3	-9.02	-60.2	-9.29	-59.6	-9.41	-58.8	-9.55	0.5	0.18
	ZK11	-53.9	-8.70	18.94			-54.1	-8.57	-54.7	-8.88	-51.7	-7.60	-57.5	-8.51	1.9	0.44
	NK9	-53.1	-8.37	12.47	-53.2	-7.87	-54.8	-8.43			-50.3	-6.54	-54.7	-8.11	1.6	0.69
	NK1	-53.5	-8.51	10.15			-53.8	-8.67					-51.1	-9.01	1.2	0.21
	JMJ-1			10.68			-54.9	-8.15			-54.4	-8.76			0.2	0.30
	JMJ-2			8.62			-51.0	-6.20			-57.1	-9.03			3.0	1.41
	CHWSQ-1			bd			-53.1	-5.82			-63.4	-9.70			5.1	1.94
	NK3-1	-56.2	-8.85	8.62	-52.5	-7.77	-48.2	-5.91			-53.7	-8.53			2.9	1.14
	NK3-2	-55.4	-8.91	12.76	-54.6	-8.54	-57.5	-8.58			-54.9	-8.57			1.1	0.15
	ZK11-2	-53.3	-8.27	9.02			-58.1	-8.77							2.4	0.25
	NK2	-53.5	-8.30	7.45			-55.3	-8.85							0.9	0.27
	NK10	-53.2	-8.56	8.21	-53.6	-8.62	-51.1	-6.78	-53.2	-8.85	-50.0	-6.91			1.4	0.90
	NHQ-1-1	-56.4	-8.78	14.02			-57.5	-8.83							0.6	0.02
	NHJ-1-2	-57.6	-9.05	13.65			-57.7	-9.39							0.1	0.17
Mountain	SDJ-1			15.39*			-52.7	-7.17			-49.9	-6.71			1.4	0.23
	Recent snow	-56.0	-10.86	19.15												
				16.11*									-59.4	-8.37		

bd-denotes below detection; Std-Standard deviation of monthly data; *Sampling time in October and December rather than April.

Table 3 ^{222}Rn and helium isotopic data of groundwater

Sam. No.	^{222}Rn(Bq/m^3)	He content (×10^{-6})	^{4}He/^{20}Ne	^{3}He/^{4}He (×10^{-6})	R/Ra
NK8	5217				
ZK06	1182	0.8	0.29	1.92	1.37
ZK05		0.7	0.29	1.83	1.30
ZK04		4.9	0.32	1.60	1.15
ZK03	18400				
NK10	14500				
ZK01	97.00	5.3	0.39	4.90	3.50
NK1	97.00				
NK9	631.0				
NK3-1	4887				
NK3-2	18000				
ZK09	2230				
NK13	49.00				

3. Results

3.1. Variability of stable H and O isotopes of groundwater

Monthly monitoring data show that temporal variations in δD and δ^{18}O values can be identified for most groundwater samples, while some of them even show large fluctuations (Fig. 3-5). A sine curve-like seasonal variation trend of δ^{18}O values for most groundwater samples can be identified (Fig. 4a), which the ^{18}O isotopes are distinctly depleted in April, September and December while enriched in July (Some of them also in June) and October. Some groundwater samples collected from shallow wells near the northern edge of the AFF or springs plot along the evaporation line in diagram of δD and δ^{18}O relationship that can be attributed to evaporation (Fig. 3 b and d). In contrast, the water table more than 10m below the surface, e.g. in the central part of the AFF (Table 1), evaporation effects of water in the aquifers are weak or absent. As a whole, there is a smaller change in δD and δ^{18}O for groundwater except for some groundwater samples show slightly positive shift particularly in δ^{18}O values. However, a distinctly positively shift for river water between April and June can be identified (Fig. 3a and Fig. 4a). With respect to April and June, the stable H and O isotopes of the most groundwater samples change to enriched and some of them relatively depleted in July, which is particularly maxima in samples collected from the northern edge of the AFF or springs and plot along the evaporation line with a small slope (Fig. 3c). However, the isotopes in river water also shows a smaller enriched variation in July with respect to June but they do not plot along evaporation line and locate left-upper area. Groundwater samples from some wells (ZK01,

ZK03, ZK04 and ZK09) in southern section and river water samples show more depleted isotopes in September after summer recharge than that in previous month in July (Fig. 3b). It seems to be followed by a return to high values in δD and $\delta^{18}O$ for most groundwater samples but more depleted values for river water samples can be observed in October (Fig 3d). All in all, values of δD and $\delta^{18}O$ in groundwater are in most cases higher than corresponding April and December values and most of them show a co-fluctuation in amplitude range with groundwater table (Fig. 4b). The most groundwater tables show small variations from April to June and distinctly rise to reach highest in September or October. The stable H and O isotopes of the most groundwater samples also correspondingly show large temporal variations after June and the largest variations can be observed in July, September, and October. The groundwater table as well as $\delta^{18}O$ values return to basic level as that of in April in December.

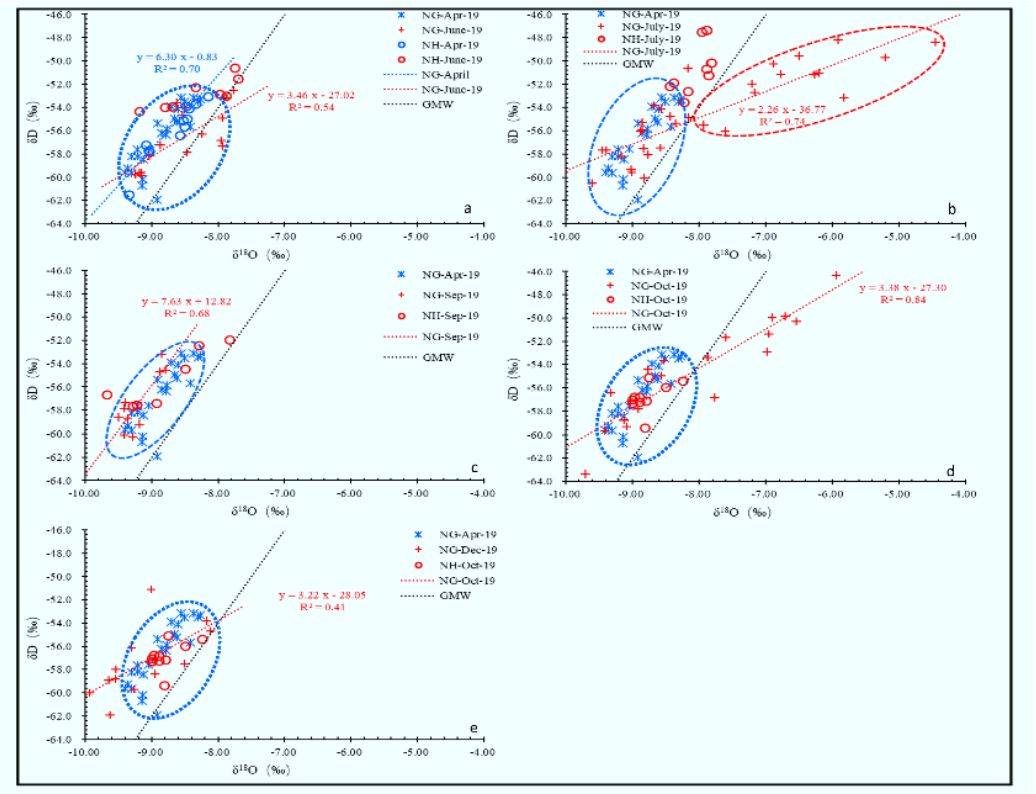

Figure 3 Diagram of the δD versus δ ^{18} O of the groundwater and river water in different months in 2019. a-June with respect to April; b-July with respect to April; c-September with respect to April; d-October with respect to April; e-December with respect to April (No river water sample is available due to freezing in December).

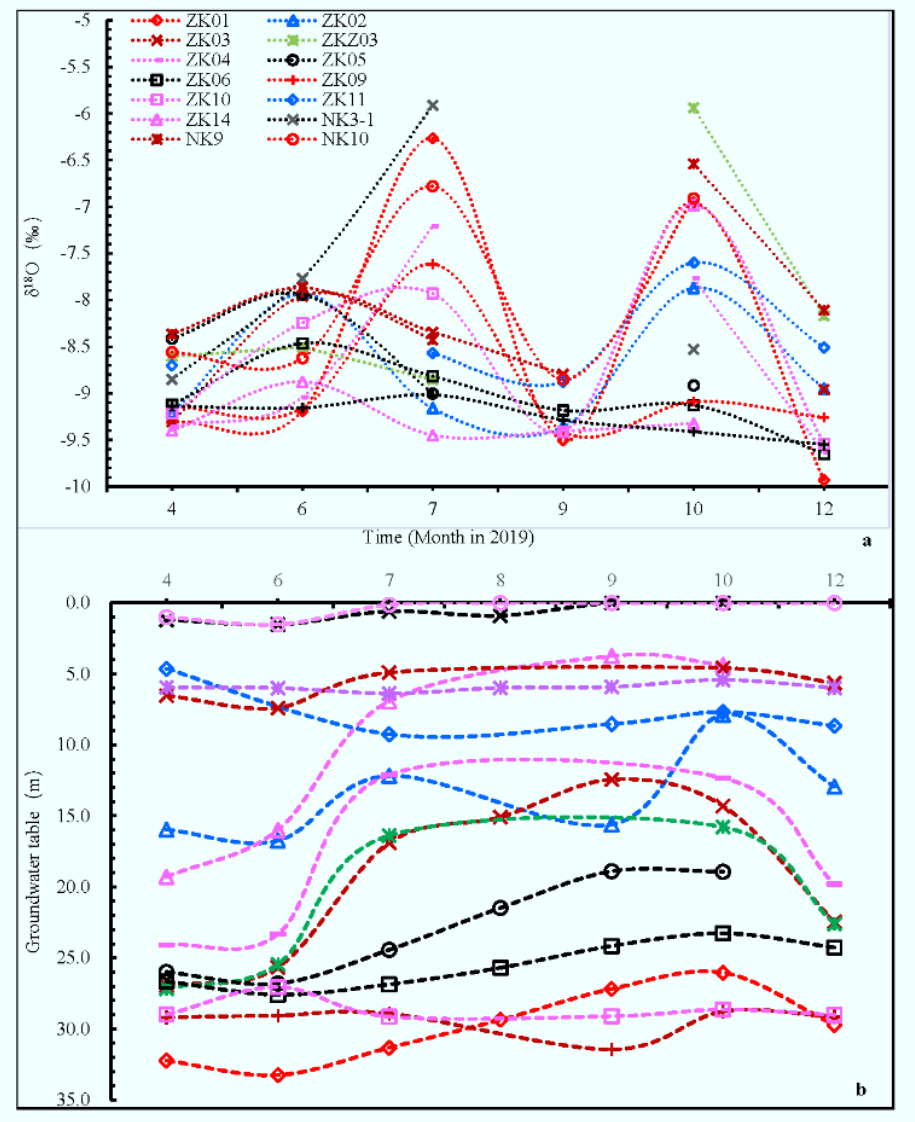

Figure 4 Seasonal (Monthly) variation of (a) stable O isotopes of groundwater and (b) groundwater table fluctuations

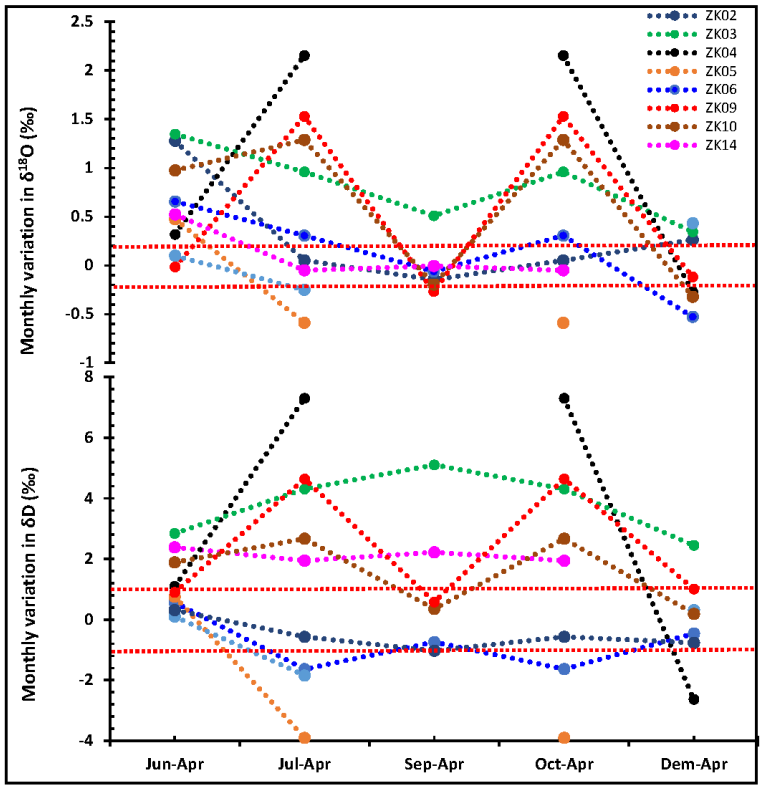

Figure 5 Monthly difference of stable H and O isotopes of groundwater. The δD and $\delta^{18}O$ values of later months (June, July, September, October and December) minus the values of April (values of base conditions). Here, the difference was selectively diagramed only for the samples with deeply buried groundwater table and distinctly monthly variations of stable isotopes. The area confined between two red dot lines denotes maximum analytical uncertainty.

From yearly variation for obtained data, groundwater samples from most wells show distinctly enriched variation trend in D and ^{18}O values from July 2012 to the same time in 2019 except for only two wells of ZK05 and NK3 (depleted). It seems that roughly similar variation trends of slopes about 2.0 from July 2012 to July 2019 for most groundwater samples can be observed in the diagram of $\delta^{18}O$ and δ D (Fig. 6). The isotopic enrichment trend is corresponding to groundwater table rising except for well ZK04. The groundwater table in the well ZK01 has risen about 28m from July 2012 to July 2019. Correspondingly, the stable H and O isotopes show greatly enriched shifts from -8.83‰ to -6.27‰ in $\delta^{18}O$ and from -57.8‰ to -51.2‰ in δ D. The large groundwater table fluctuations associated with distinct stable isotopic variations in the annual-scale can be also observed in the AFF of NR catchment.

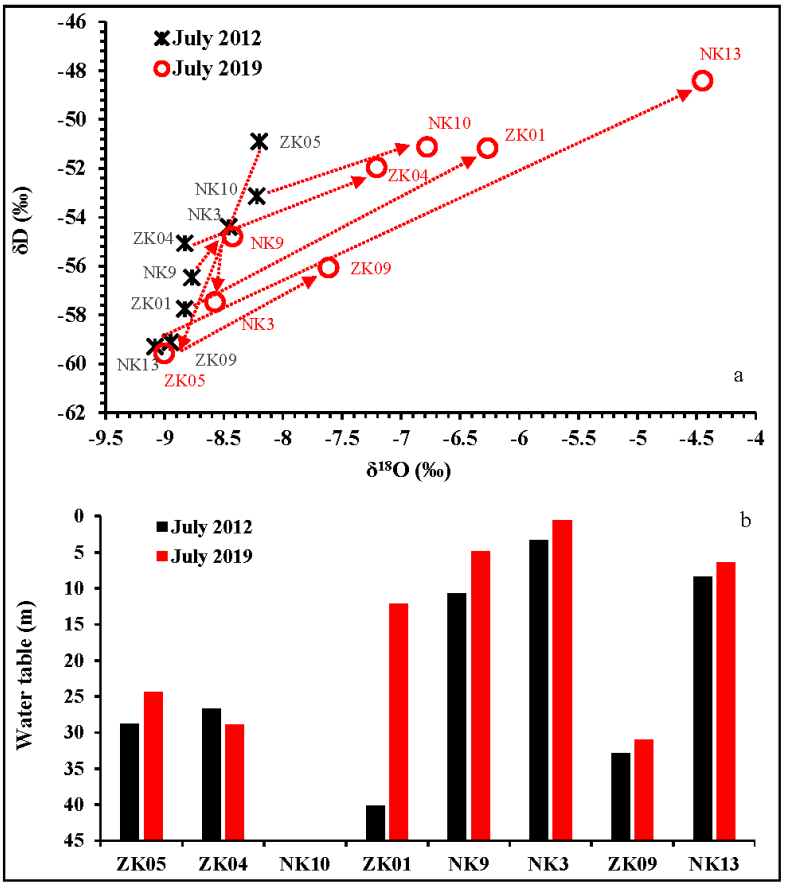

Figure 6 The variation trend of stable H and O isotopes and groundwater table fluctuation of wells between in July 2012 and 2019. From the diagram, the most groundwater tables show a rising trend while stable isotopes positive shift.

3.2. Distribution characteristics of other isotopes (T, He and ^{222}Rn) of groundwater in dry season

Almost all groundwater samples in the AFF of NR catchment show high content of tritium except for one sample from confined artesian well in the foreland nearby the fluvial plateau (CHWSQ-1 in Table 2). The T content in groundwater ranges from 7. 5TU to 19.1TU. Samples from river water show higher T content with smaller variations (15.3-17.7TU) and are similar to recent snow samples (16.11 to 19.15TU). There are no previous T data available for the NR catchment, but are similar to high tritium values reported in the neighboring Golmud River water, groundwater and precipitation if they are corrected by 28 years radio-active decay (Sun et al., 1991). The tritium content in groundwater or river water in the NR catchment is higher than that of modern

precipitation elsewhere in the northern hemisphere, where the tritium content varies between 5 and 12 TU (Morgenstern et al., 2010; Chae et al., 2019), but is close to the range of precipitation monitored in the northeastern Tarim Basin (Zhao et al., 2019) and is also close to the most recent measurements reported by the IAEA for Zhangye and Wulumuqi at about the end of the pulse of anthropogenic tritium in western China (http://www.univie.ac.at/cartography/project/wiser/). In addition, the precipitation in Tianshan Mountains and Qilian Mountains all correspondingly show high T content (Kreutz et al., 2003; Zhao et al., 2018), which indicate the NR catchment is located a typical area with high modern background T content of precipitation. There seems to be no regular spatial variation law of T content in groundwater of NR catchment, e.g. the distance from river bed or mountains and deep or shallow groundwater.

Four typical groundwater samples (Table 3) show the similar ratios in $^{4}He/^{20}Ne$ but larger variations in content of He and ratio of $^{3}He/^{4}He$. the groundwater samples collected from the center of AFF (ZK01 and ZK06) show higher $^{3}He/^{4}He$ ratios. In particular, the groundwater in well ZK01 shows a very high content of He (5.3×10^{-6} v/v) as well as the highest $^{3}He/^{4}He$ ratio (3.5Ra). The $^{4}He/^{20}Ne$ ratio in this groundwater sample is also high. Thus, the high $^{3}He/^{4}He$ ratio should be related to the high content of ^{3}He rather than low content of ^{4}He. The other groundwater samples also have $^{3}He/^{4}He$ ratios higher than 1Ra, the atmospheric rate, which suggests addition of deep-circulating water enriched in ^{3}He.

The content of ^{222}Rn in the groundwater in AFF of NR catchment shows a large variation from 49 to 18400Bq/m^3. If the lowest content of 49 Bq/m^3 (well NK13) in the whole catchment is regarded as local background value of groundwater, most groundwater samples show hundreds or even thousands of times higher content than local background (Table 3). This also suggests the presence of groundwater as circulated through underlying bedrock.

4. Discussion

4.1. Temporal recharge source and renewal of groundwater system

4.1.1. The law of spatial and temporal fluctuation of the groundwater table

Different from a general arid basin, the groundwater table of thick aquifers developed in AFF of NR catchment shows significant temporal variations, both in interannual, monthly, daily and hourly time scales, respectively (Fig. 7a, b and c). There are almost no human activities to affect the groundwater system, and the water table mainly fluctuates under natural conditions. Firstly, as to

the interannual time scale, the groundwater table in almost all wells distinctly rises during the wet season from June to September (sometimes extending into October) and then, declines again after following October each year. The groundwater table increases to reach the highest in September or October while it drops to the lowest in April or May with also a sine curve-like fluctuation. During strong recharge seasons, the groundwater table successive rising trend can be observed on daily and even hourly time-scales. The groundwater table in wells ZK01, ZK03, ZK05 and ZK06, showed a distinctly rising trend from July 1st to 31st in 2019 as well as within 72 hours from July 14th to July 16th (Fig. 7b and c). These rising fluctuations of the groundwater table in different time-scales indicate rapid water recharge processes occurring during the wet season. The groundwater table fluctuates every year, but concerning previous years, the groundwater table in most wells have distinctly upwelled to reach the highest level for ten years in September to October 2019. For example, the groundwater tables in wells ZK03, ZK01 and ZK05 have risen each year from 2010 to 2013 between July and September 12.38m, 10m and 5m, respectively. Most shallow groundwater levels have even reached the surface or discharge as springs in the northern edge of AFF, indicating that the recharge water amount or storage of groundwater have been increasing a lot since 2013 in the NR catchment. The analysis of GRACE data also concluded that water storage has distinctly increased in QB in recent years (Jiao et al., 2015; Xiang et al., 2016). From the seasonal time scale in 2019 (Fig. 4b), the monthly groundwater table variation is similar to previous years with a distinctly rising trend in the wet season while declining in the dry season. Most wells with deeply buried groundwater table in the southern monitoring section (around the centre of AFF) also show distinctly rising trends after recharge since April. Groundwater tables in the well ZK14 nearby the mountain front and ZK03 adjacent the mainstream rose from April to September close to and over 15m, respectively. The groundwater table in ZK03 and ZK01 rose within one-month over 2m and over 5m, and about 0.1 to 0.5m within 72 hours in July, respectively (Fig. 7b and c). Reversely, a few wells around the Hongxing Water Supply Company (No. ZK11、ZK09、NK13 and ZK10) do not show a distinctly rising trend of the groundwater table in summer and even some decline, which should be related with increasing anthropogenic freshwater extraction counterbalancing the natural rising trend on a local scale.

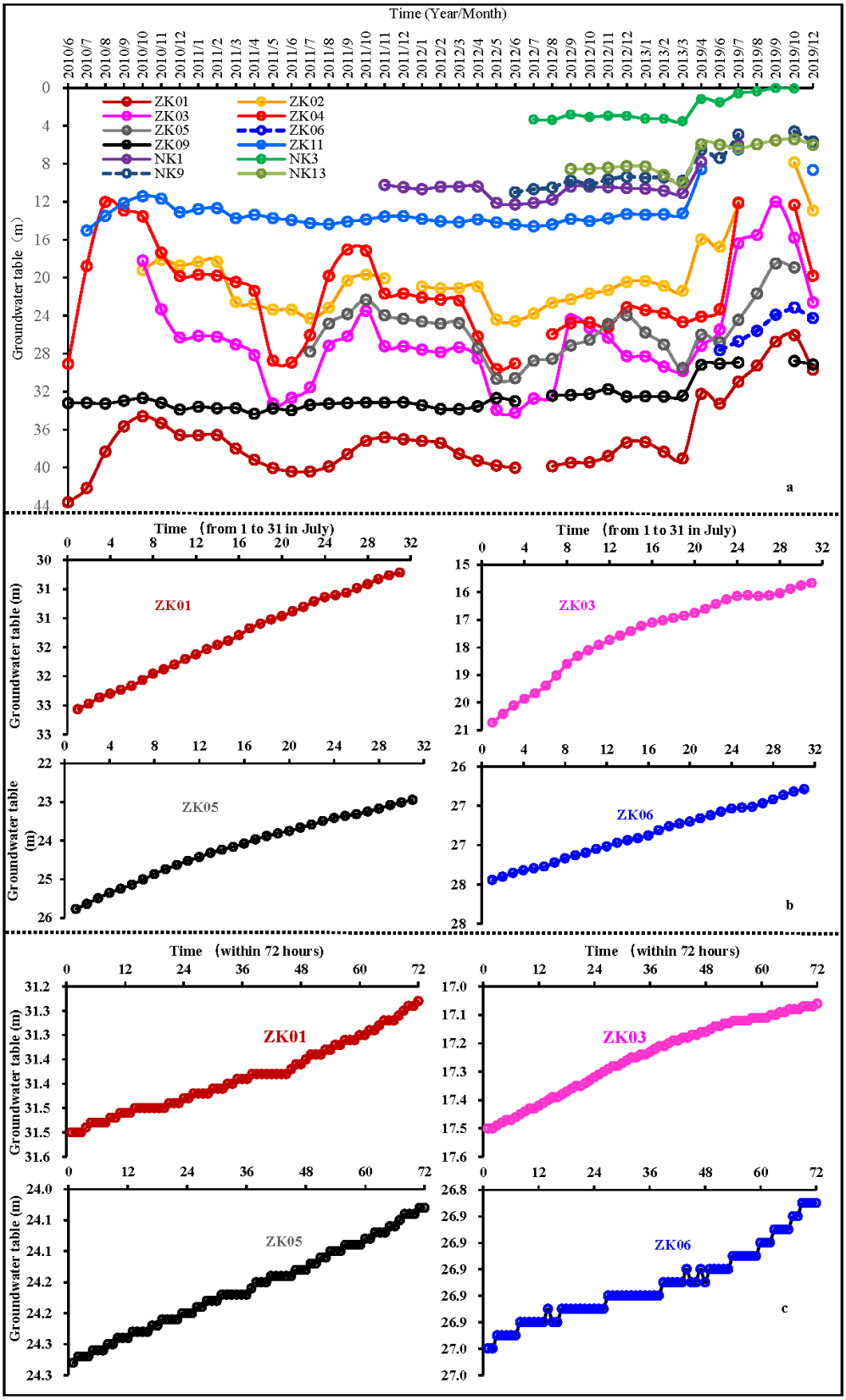

418

419 **Figure 7** Groundwater table fluctuations in the time-scale of (a) year/month, (b) day/month and (c)
420 hour/day in the AFF of NR catchment (Data within 72 hours recorded from 14 to July 16th 2019
421 using high-precision automatic water gauge (HOBO U20 Ti).

From the spatial variations of groundwater table, the wells with more significant dynamic fluctuations mainly distribute around southern monitoring section and close to mountains, where the well ZK14 nearby the mountain front show the most considerable monthly groundwater table difference. Also, the wells ZK03, ZK04 and ZKZ03 located nearby and ZK05 or ZK06 far away from the mainstream show a more substantial groundwater table fluctuation of a rising trend after April. The monthly fluctuation of groundwater table becomes smaller and smaller from the mountains to the northern edge of the AFF, which is corresponding to a general catchment. However, the different characteristic from a general mountain-river-basin system is that groundwater table fluctuation seems to be no natural law with the distance from the mainstream. Generally, the closer to the mainstream is, the more substantial variation of groundwater table occurs for river water regularly infiltrates to recharge groundwater when flows across the AFF. That is, the groundwater table will relatively maintain stable due to the slower recharge and longer renewal time if it is far away from the mainstream or river channels. However, there seem to be no corresponding tight relationships between groundwater dynamics and distance to the significant river channel in AFF of NR catchment. This unusual scenario is related to individual preferential conduits for groundwater recharge through faults or other structures in the mountains rather than only dependent on river water infiltrating through unsaturated zones in the basin. The mechanism will be discussed in later sections.

At present, the groundwater dynamics are mainly governed by a natural recharge and discharge balance in the NR catchment. The distinctly rising groundwater table during the wet season in the thick aquifers in the centre of the AFF (with water table buried over 10m or 20m, respectively) indicates favourable circulation conditions of the groundwater system and bears great significance for water resources exploration in the future. Moreover, the interannual groundwater table fluctuation law in the NR catchment is not only the response for seasonal climate changes every year but also as a response to constant climate warming in the last ten years.

4.1.2. Water source inferred from temporal variability of stable H and O isotopes

Previous results show that the stable H and O isotopes in groundwater for most wells in the AFF of the NR catchment display distinct or identified temporal variations, particularly seasonal effects also display sine-like curves corresponding to groundwater table fluctuations (Fig. 4 and 5). Thus, the rising groundwater table and corresponding variations in stable isotope records during the

wet season argues for water recharge and at least partly renewal of old water in the aquifers. Some groundwater samples from wells or springs located near the northern edge of the AFF display different intensities of evaporation effects for the shallow groundwater table and δD and $\delta^{18}O$ obtained within plot along the evaporation line (see Fig. 3 b, d). Groundwater samples from wells in the centre of the AFF and nearby the mountain front plot in the upper-left area of the global meteoric water line (GMWL), arguing for a local continental derived source. This scenario is widespread in the groundwater circulation system in the high-cold Tibetan Plateau (Li et al., 2020). Kong et al. (2019) concluded that non-monsoon precipitation, sourced from inland glaciers on the Tibetan Plateau, govern the groundwater recharge in the foreland basin, where the local monsoon precipitation, sourced from the ocean, plays negligible effects. The groundwater recharge in the exceptionally arid QB basin should further follow this trend as it receives only scarce precipitation. The primary recharge source therefore originates from precipitation of local moisture circulation patterns in the high elevation of the eastern KM, where waters can directly infiltrate and recharge the groundwater and rivers.

In the dry season in April, the groundwater table drops to reach the lowest state and stable H and O isotope compositions in the groundwaters are relatively lighter (than values obtained later in the year) and plot close to river isotopic compositions. Consequently, both the river and groundwater, reveal similar a source, i.e. the discharge of groundwater in the mountains as the base flow of the NR. During winter in the permafrost region, nearly the entire river base flow is contributed by groundwater discharge (Liu et al., 2012). Until June, the glacial-snow meltwater shows greatly increasing trends, however, significant precipitation does not occur. Following Sergey et al. (2009) snow sublimation causes kinetic isotope fractionation leading to an enrichment in heavy H and O isotopes in the meltwaters. Consequently, the H and O isotope compositions of rivers fed by meltwaters should become isotopically heavier than that in April. However, the isotope compositions in groundwater in AFF show no significant variations between April and June, despite the groundwater table rising (Fig. 3a). This suggests that the proportion of new recharge water in the aquifers may be too small for significant impact on the isotopic compositions, or new recharged water hasn't reached the aquifers in the AFF within two months' lag time. From July, temporal precipitation occurs occasionally, while the glacial meltwater flux increases to its largest level and evaporation is the strongest. For wells or springs near the northern edge of the AFF, evaporation causes H and O isotope fractionation towards heavier values recorded in the groundwater (Fig. 3b).

Most groundwater samples plot along the evaporation line with a good linear relationship (R^2=0.74). The negative end-member is defined by groundwater samples from the centre and the southern area of the AFF. A trend line fitted through samples from near the northern edge of the AFF reversely extends to the left-lower corner, which means that the groundwater developed in the centre and southern area, as well as the northern edge of the AFF, have a similar source. The groundwater flows from the center to the northern AFF and surface discharge as springs and in swamps or wetlands. Thus, here it only needs to trace the source of groundwater in the centre of AFF for weak or negligible evaporation effects on stable isotopes. Concerning April, the distinct enriched shift in stable H and O isotopes in the groundwater and river, as well as rising water table in the AFF in July (Fig. 4), suggest juvenile water input into the aquifers. The new water should originate from upper reaches of the NR with heavier isotopes (sample No. NH7 and NH8) as well as meltwater from high elevation vertical infiltration. The groundwater table gradually rises to reach the highest level in September and October after successive recharge during the wet season (Fig.7). The rising groundwater table makes the most areas become a swamp in the northern edge of the AFF making the research area inaccessible from September on. According to recent three years' monitoring data in the source region of the Yangtze River (Li et al., 2020), the precipitation dominates and accounts for 48% of runoff with the maximum temperature and precipitation occurring and stable H and O isotope compositions changing to lighter values in August. The climate is similar in the source area of the NR with the source region of the Yangtze River. So, although there is no precipitation sample available, the distinctly depleted H and O isotopes in the groundwater in September in the AFF of NR catchment should be more likely caused by replenishment of mountain precipitation from July to September. Compared to April, the groundwater in October exhibits distinctly heavier H and O isotope compositions (Fig. 3c). In particular, the groundwater samples from the northern edge of AFF in October also show distinct evaporation effects in H and O isotopes and samples plot along the evaporation line with an obvious linear relationship (R^2=0.84) (Fig. 3d). The negative end-member of reversely extensive evaporation line is also very close to samples from the centre of the AFF. Considering the rising by a wide margin of groundwater table in September and October, the successive recharge since July correlates to a response at the end of the wet season. The stable H and O isotopes in groundwater in the centre AFF changes to relatively enriched and is closer to river water. In contrast, the groundwater table gradually drops after October. The reason why the groundwater table naturally declines and gradually recovers to its base condition is mainly attributed

to a large water discharge at springs in the edge of the AFF as well as laterally runoffs into the northern lakes, indicating that the groundwater system fully adjusts after the strong recharge during the wet season. The stable H and O isotopes of groundwater in December return to base values like in April with recharge source water changes to base flow (mainly fed by spring water) in the mountains.

Due to the very complicate nature of water source compositions and seasonal variations in a high-altitude cold-climate mountains and basin system, it's hard to estimate the large seasonal proportion of groundwater accurately. Here, some typical wells with deep groundwater table (>20m) and sizeable seasonal water table fluctuations (>5m), as well as identified seasonal variation of stable isotope compositions, were selected to statistically estimate the recharge proportion of the groundwater system during the wet season from June to September. The groundwater in June can represent the beginning of large-scale recharge. The groundwater in September can be regarded as a mixture of new and old water after substantial recharge. Then, the recharge proportions of groundwater can be estimated using the isotope mass balance equation:

$$f\times\delta^{18}O_r+(1-f)\times\delta^{18}O_g=\delta^{18}O_m$$

where $\delta^{18}O_r$ denotes for the isotopic composition value of the main recharge source water during the time from June to September (-9.47‰, average river value of the upper NR before flowing out the mountains in September). $\delta^{18}O_g$ denotes for the old groundwater isotopic end-member contained in the aquifers in June (-8.58‰, averaging data for groundwater of wells with table rising over 5m in the centre of the AFF), $\delta^{18}O_m$ denotes for the isotopic composition of the mixture of groundwater in September (-9.24‰, averaging data for groundwater of the same wells as in June), and f indicates the mixing proportion (%). The calculation results show that the river water proportion in the mix is in the order of 68% while old water accounts for the remaining 32%. Therefore, 68% groundwater was replenished during the wet season from June to September in 2019 for groundwater samples with large water table fluctuations in the centre of the AFF of the NR catchment. It is that large proportion of new water added in the aquifers that drives the groundwater table to rise up to 15m

after recharge during the wet season.

4.1.3. Replenished period and estimated age of groundwater inferred from isotopes and water table

Almost all wells show high contents of T in the groundwater except for one confined groundwater sample collected in the northern edge of the AFF of the NR (Table 2). The T content in most groundwater samples matches river concentrations. Two typical wells (ZK10-11) with the highest T content have very rich groundwater with water yields of more than 5000m^3/d (data from the pumping test), denoting for excellent circulation conditions in the groundwater system. There has been no T released by new atmospheric thermal nuclear tests since the Comprehensive Nuclear Test Ban Treaty in the 1990s. All the river water samples in the NR show higher T content than 15TU and are close to recent snow meltwater concentrations of 19.15TU (Fig. 8), suggesting that the river water even at base flow state in April mainly originates from current precipitation. The T content in the adjacent Golmud River ranged from 84 to 123TU in 1987 and from 42.6 to 67.0TU during rainfall in 1998 (Sun et al., 1991). All these datasets exhibit a distinct higher background T content. According to the radioactive decay law, current precipitation should have T contents ranging from 14 to 21.96TU, which overlaps with recent snow meltwater concentrations (19.15TU). The T content is also close to concentrations obtained during a precipitation event in 1998 if it is assumed that the river water in 1987 can represent the current meteoric water and further experienced about ten years' of radioactive decay. All these facts approve that the T content in the river water can roughly describe the background value of the current precipitation. So, the groundwater samples with high T content (closing to content of river water) should be recently recharged and the renewal period may probably be limited within yearly or even seasonal time scale (Fig.8). In contrast, the groundwater sample with the second-highest T content (10-15TU) mean that relatively older water, recharged several years ago, likely occupies a more substantial proportion. The circulation period should be within 0 to 12 years with less than a half-life of tritium. The very young groundwaters with higher T contents (over 10TU) are mostly located in the centre or southern area of the AFF. In addition to higher T content, the circulation period for other groundwater samples with relatively general T content (5-10TU) may be probably recharged over ten years but less than two half-lives (within 24 years) or even older. There seems to be no natural variation law of groundwater replenished period in the the AFF except for a very young age in the mountains and

relatively older age in the alluvial plains. Almost all groundwaters developed in thick aquifers of the AFF in the the NR catchment (over 150m or 250m in depth) should be very young and can be classified as a modern groundwater circulation system.

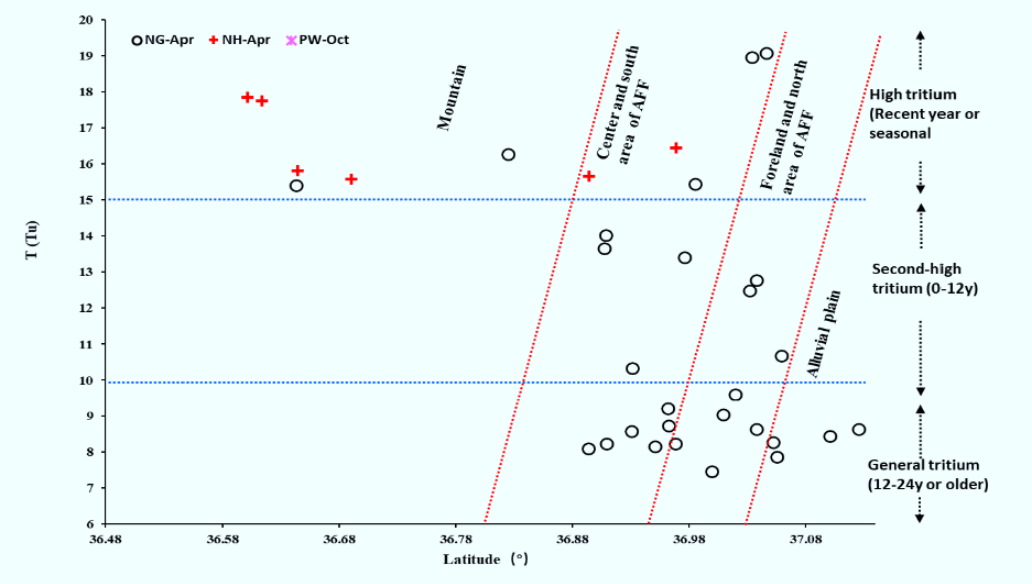

Figure 8 Estimated replenished period of groundwater systems from Mountains to Basin in the Nalenggele River catchment (NG-Apr denotes samples of groundwater in April; NH-Apt denotes samples of the river in April; PW-denotes snow samples collected from mountains in October)

4.2. Conceptual model of the hydrological processes controlling rapid groundwater circulation system

Generally, river water can infiltrate to recharge groundwater through loose alluvial or fluvial deposits when it flows out of mountains into the basin. However, there is no adequate river water to recharge groundwater and to account for a groundwater tables' monthly rise by several meters or decameters. Over 70% of the NR water is lost in the mountains, and it is almost completely evaporated after flowing out of the mountains during the dry season. Besides, it should be a long time only dependent on water to infiltrate through thick vadose to recharge groundwater. Thus, there might be a mechanism governing the rapid recharge and circulation of groundwater forming abundant groundwater resources in the the AFF of the NR catchment.

As an area with intense tectonic and volcanic activities in the mountains as well as a very young groundwater system with rapid recharge and circulation in the AFF of the NR catchment, the unusual high $^{3}He/^{4}He$ ratios in the groundwater are more likely related to deep fluids or upwelling

mantle de-gassing. Previous studies concluded that the formation of unique salt-lake resources with extreme enrichments in B, Li and other incompatible elements as well as high concentrations both in rivers and groundwater in the NR catchment might be mainly sourced from deep fluids (Tan et al., 2012). The high content of ^{222}Rn in the groundwater further indicates the development of faults or other large-scale fractures effecting the groundwater circulation system. The groundwater in some wells in the centre of the AFF of the NR shows a large groundwater table rising trend in the wet season as well as distinct stable H and O isotopic variations and high content of T. All these characteristics correspondingly suggest favorable structures as conduits developed for groundwater rapid recharge and circulation.

Generally, water flow in crystalline basements is enabled by the occurrence of interconnected fracture networks (Bucher and Stober, 2010) and the presence of hydrological driving forces (Ingebritsen and Manning, 1999). Mountain topography has been long ago recognized as a critical driver for precipitation deep and long-distance circulation. The tectonic, topography and geomorphological characteristics are special in the upper or source area of the NR, which are very different from the general river catchment. As a centre of collision and convergence of the Altyn Mountains and the Kunlun Mountains, a series of deep and large-scale faults and many kinds of volcanic craters have been developed (Fig. 2). Besides, recent intense tectonic activities, the Kunlun Mountains are still rising, while the QB is relatively declining (Wang et al., 2012; Zhou et al., 2018). A massive earthquake (Ms 8.1) happened on November 14th 2001 along the NWW slip fault belonging to the eastern Kunlun fault zone. Geological investigations found that a 350km-long left-lateral rupture zone with a maximum left-lateral displacement over 6m have been developed since the earthquake (Yin et al., 2002). Klinger et al. (2005) concluded that the earthquake ruptured a 450-km-long stretch of the sinistral Kunlun strike-slip fault, at the northeastern edge of the Tibet plateau. These young (Quaternary) deep faults cut through the source area of the branch of HR catchment, which has developed very significant hydrothermal activity and deep fluid circulation (Tan et al., 2012). Moreover, frequently occurring volcanic activity developed many kinds of craters in ancient times, with the latest eruptions in 1952 and 1984 in the source area of the NR (Zhu, 1989). Thus, the favorable conduits have been developed in the source area and the upper NR (including HR and CR branches) under the background of these tectonic and volcanic activities (Fig. 9). The high content of ^{222}Rn and $^{3}He/^{4}He$ ratios indicate deep fluids or gas can move upward to reach the shallow aquifers. These profound substances can generally move upward along deep faults. Thus, a

unique condition of groundwater circulation system in the NR catchment is that, in addition to general conduits for shallow groundwater circulation, the active significant faults or craters can be well acted as favorable conduits for deep groundwater circulation. This is furtherly certified by considerable enrichment of elements of B and Li (over ten times higher than general freshwater) in the very fresh groundwater as well as large-scale B and Li resources developed in the tail salt lakes (Tan et al., 2012).

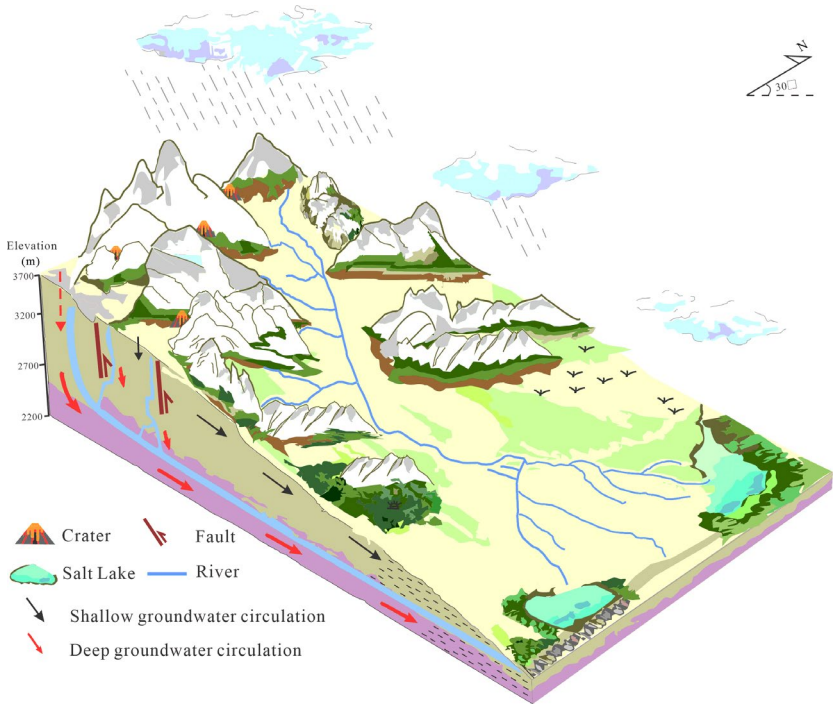

Figure 9 Conceptual model indicating the rapid groundwater circulation process in a typical high-cold mountain-arid basin system

In addition to excellent conduits for groundwater recharge and runoff, the plentiful water sources and large water head fall from source to aquifers in the AFF of NR catchment are also an essential critical condition to drive rapid surface water to groundwater recharge and underground circulation. Large-scale glacial and snow cover the northern slope of the eastern KM where abundant summer precipitation occurs as well. The steady flow of glacial-snow meltwater and temporal precipitation supply are an adequate water source both for the NR and groundwater. In particular, the elevation in the source area of the high mountains is over 4000-5000m a.s.l. while it declines to lower than 2900m in the principal aquifers of the AFF of the NR. Thus, these abundant source waters in the high mountains can vertically and rapidly infiltrate along favorable conduits

(significant faults and crater) and then laterally move along all kinds of structures including shallow pores within loose sand-gravel deposits to recharge groundwater in the AFF under over 1000-2000m water head fall. Overall, the abundant water source yielded in high mountains, favorable conduits of significant faults and craters in the mountains and macropores developed in shallow sands or gravel strata in the middle-lower reaches. Excellent water head difference from the source area of high mountains to aquifers in the lower basin combinedly drive and maintain the rapid recharge and circulation processes of groundwater all the round between high-cold mountains and low basin system. As for such abundant groundwater resources developed in the AFF of NR catchment, in addition to above preconditions, it is also related to very thick aquifers over 100m to 200m with sands-gravel deposits, which supply adequate space for groundwater storage.

Based on the rough water budget, local hydrological observations conclude that enormous quantities of groundwater resources have developed in intermontane basins of upper-middle reaches of the NR catchment for over 70 percent of the river water infiltrated to recharge groundwater before the river flowing out of the mountains (Wang et al., 2008). The conceptual model of the hydrological processes of groundwater circulation between the mountains and basin in the NR catchment issued in this study furtherly believes it a reasonable presumption. Moreover, it seems to be much likely that there have collections between groundwater system in intermontane basins at higher elevation and groundwater in QB at lower elevation through underground conduits.

4.3. Trend prediction on groundwater table fluctuation and storage

Many previous studies approved that the climate warming is very distinct on the Tibetean Plateau and the QB is one of the areas with the most substantial temperature rise (Jiao et al., 2015; Xiang et al., 2016; Kuang et al., 2016). From the meteorological records (since 1956) of trendline of annual temperature and total precipitation variations in Golmud station nearby research area (Fig. 10), the precipitation displays large-scale fluctuations for different years, and the fitted linear trendline is not very distinct (R^2=0.14). A weak, increasing trend of rainfall since 1956 can be identified. In contrast, a very definite rising trend of temperature with an excellent linear correlation (R^2=0.85) can be observed. The average rise in temperature is in the order of 0.06℃/year over the past 60 years. The temperature has never dropped to be lower than 4℃ since 1970 and maintained over 6℃ in the recent 20 years. Successive warm climate might be expected to accelerate the shrinkage of glaciers and permafrost and increase the availability of water in the source or upper

NR catchment. The more enriched in stable H and O isotopes in the groundwater as well as water table rising in July 2019 than that the same time and same well in 2012 in the AFF of NR catchment may be more likely related to the response of this hydrological process (Fig. 6). The response mechanism governing the distinctly enriched stable H and O isotopic variation in groundwater needs furtherly to be tracked. It possibly indicates that the recharge water proportion from glacial melting of permafrost releasing increases under the effect of climate warming. The evaporation and sublimation processes in snow, ice and permafrost samples shows significant fractionation in observed $\delta^{18}O$ and δD in residual meltwater (Sergey et al., 2009). This means that the proportion of meltwater from remaining snow or ice and permafrost releasing water after a long time of evaporation (and associated sublimation) increases in the groundwater for successive climate warming from 2012 to 2019. Besides, the precipitation will also increase in the high mountains with temperatures rising in the area. For example, in the Qilian Mountains, the contribution of recycled moisture to rainfall increased by 60% since 1990, which has increased runoff and changed seasonal runoff patterns and runoff components (Li et al., 2020). Thus, the total water in the recharge area will increase significantly with glacial-snow-permafrost meltwater and temporal precipitation increasing.

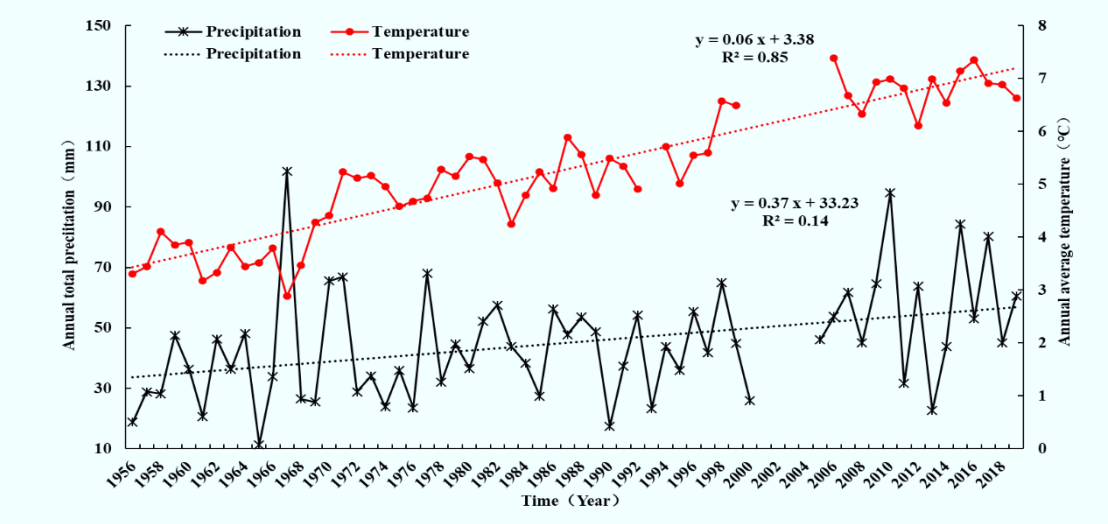

Figure 10 Meteorological records (trendline of annual temperature and total precipitation variations) from Golmud station nearby Nalenggele River catchment.

Although there are no long-term monitoring records in the mountains for hard natural conditions, sporadic monitoring data found that over 70 per cent of the river water infiltrated to

recharge groundwater before the river flowing out of the mountains (Wang et al., 2008). Field observation of this study in 2019 also noticed that the runoff of two upper main branches of CR and HR had a substantial quantity of water at the end of spring and summer. Still, most of the water lost after flowing out the mouth of mountains and the river was almost dried up in the basin. This means that the groundwater in the AFF of NR catchment mainly receives recharge from lost surface water in the mountains rather than the recharge from river runoff in the basin. Thus, it can be well predicted that the groundwater table will substantially rise if the total water in the mountains (recharge area) increases with the successive climate warming expected in the future. Moreover, a large reservoir has been building in the NR at the mouth of mountains in future ten years. The rising trend of groundwater table will be more accelerated for the recharge water will increase driven by the hydraulic pressure increasing when much more water is retained in the reservoir. The rising groundwater table will increase the water storage and yield more water resources for the QB while it will also result in potential natural hazards. The substantial rising groundwater table will easily incur serious salinization and alkalinization in the extremely arid basin. Besides, the oasis located in the northern edge of AFF will much likely be perennially submerged into water and lose the natural ecological function due to much more water discharged under groundwater table rising. The tail Salt Lake resources (K, B and Li minerals) will also be affected by increasing discharge water. Therefore, the exploration of water resources in the NR catchment cannot only become dependent on surface water in the future with facing climate changes. The exceptionally rapid groundwater circulation characteristic between the high-cold mountains and arid basin system impels the practicable development of superior groundwater resources. The development and utilization of rich and excellent groundwater resources in the AFF of NR catchment must control a reasonable scale, which can abstract water to satisfy other town or cities with water resources scarce but large-scale demands, such as adjacent Golmud city and northern QB, and while must maintain groundwater table fluctuates in a balance or reasonable dynamic state and prevent it from over rising.

5. Conclusions

1) A distinct seasonal or monthly fluctuation of groundwater table as well as identified stable isotopic variations can be observed in the AFF of Nalenggele River catchment in Qaidam Basin. The large-scale rising groundwater table with identified stable isotopic variations during the wet season indicate the large proportion of seasonal renewal of groundwater occurring. The recharge

source of groundwater in the fan mainly originates from surface water vertical infiltration in the Kunlun Mountains.

2) Both the river and groundwater have a high concentration of radio tritium, which the content is very close to current precipitation. Combining high content T with the association of significant seasonal groundwater table dynamics and stable isotopic seasonal effects, the age and renewal rate of groundwater should be very rapid. The groundwater seems to be very young with recharge age about 0-12 years for aquifers developed in the centre and near the mountain front or mountains and about 12 to 24 years in the northern edge of the AFF of NR catchment. Some confined groundwaters with almost free T content in the alluvial-fluvial plateau may be over 60 years before recharge and need to be furtherly approved.

3) The mechanism governing the formation of abundant groundwater and rapid circulation in the AFF in extremely arid Qaidam Basin may be mainly related to several favorable hydrological conditions. Firstly, the plentiful water from glacial-snow melt and temporal precipitation in the high mountains supply adequate recharge source. Secondly, large-scale active faults and volcanic craters and other macro-structures can be acted as favorable conduits to drive abundant source water to infiltrate and laterally runoff vertically. Thirdly, the massive hydraulic head, over 1000-2000 m, appears to rapidly drive infiltrated water flow over distances from recharge area in high mountains to the alluvial-fluvial fan. Finally, the very thick loose sands and gravel strata over 100 or 200 m supplies enough groundwater storage space in the basin. Thus, the rapid groundwater circulation system and affluent groundwater resources can also be developed even in the very arid basin far away from the recharge area.

4) The successive warm climate in the future might be expected to accelerate the shrinkage of glacial and increase precipitation in the high Kunlun Mountains. As a response, the trend of groundwater table in the AFF of NR catchment will rise more rapidly and dramatically with recharge water increasing in the source area. Thus, it will supply more superior water resources for arid Qaidam Basin as well as prevent oasis and soil from salinizing and alkalinizing if groundwater in the alluvial-fluvial fan is reasonably explored in the future.

ACKNOWLEDGMENTS

We are grateful to professor Christopher J. Eastoe and Dr. Simon Hohl for final grammatical and professional editing. We also appreciate many workers who helped to collect samples through

abstracting water from wells. This study was financially supported by the National Key Research and Development Program of China (2018YFC0406601) and National Natural Science Foundation of China (41872074). All data used in the work is available at table 1, 2 and 3 inserted in the text. For more detailed information regarding the data, please contact Hongbing Tan (tan815@sina.com). The meteorological data used in figure 10 is available at weather for 243 countries of the world: https://rp5.ru/Weather_in_the_world.

References

Aude, V., Sophie, V., & Guðfinna, A. (2019). Groundwater in catchments headed by temperate glaciers: A review. Earth-Science Reviews 188, 59–76. https://doi.org/10.1016/j.earscirev.2018.10.017

Bucher, K., Stober, I., (2010) Fluids in the upper continental crust. Gefluids, 10, 241–253. https://doi.org/10.1111/j.1468-8123.2010.00279.x

Bijeesh, K.V., Wang, S.S., Sergio, F. S., Ulisses, F.B., & Jefferson, C.S. (2017). Glacier monitoring and glacier-climate interactions in the tropical Andes: A review. Journal of South American Earth Sciences, 77, 218-246. https://doi.org/10.1016/j.jsames.2017.04.009

Currell, M.J., Cartwright, I., Bradley, D.C., & Han, D. (2010). Recharge history and controls on groundwater quality in the Yuncheng Basin, north China. Journal of Hydrology, 385, 216–229. https://doi.org/10.1016/j.jhydrol.2010.02.022

Clarke, I., & Fritz, P. (1997). Environmental Isotope in Hydrogeology, Springer-Verlag, Lewis Publishers, New York, https://doi.org/10.1007/s00254-002-0677-x

Chae, J.S., & Kim, G., (2019), Seasonal and spatial variations of tritium in precipitation in Northeast Asia (Korea) over the last 20 years. Journal of Hydrology, 574, 794–800. https://doi.org/10.1016/j.jhydrol.2019.04.058

Chen, Z.Y., Qi, J.X., Xu, J.M., Ye, H., & Nan, Y.J., (2003). Paleoclimatic interpretation of the past 30 ka from isotopic studies of the deep confined aquifer of the North China plain. Applied Geochemistry, 18, 997–1009. https://doi.org/10.1016/S0883-2927(02)00206-8

Chen, J.S., & Wang, C.Y. (2009). Rising springs along the Silk Road. Geology, 37, (3), 243-246. https://doi.org/10.1130/G25472A.1

Chen, H., Zhu, Q., Peng, C.H., Wu, N., Wang, Y.F., Xiu Q.F., et al. (2013). The impacts of climate change and human activities on biogeochemical cycles on the Qinghai-Tibetan Plateau, Global

791 Change Biol, 19(10), 2940–2955, https://doi.org/10.1111/gcb.12277
792 Gleeson, T., Befus, K.M., Jasechko, S., Luijendijk, E., & Cardenas, M.B. (2016). The global volume
793 and distribution of modern groundwater. Nature Geoscience, 9, 161–167. https://doi.org/10.1038/
794 ngeo2590
795 Gates, J.B., Edmunds, W.M., Darling, W.G., Ma, J., Pang, Z., & Young, A.A. (2008). Conceptual
796 model of recharge to southeastern Badain Jaran Desert groundwater and lakes from environmental
797 tracers. Applied Geochemistry, 23, 3519–3534. https://doi.org/10.1016/j.apgeochem.2008.07.019
798 Glenn, E.P., Scott, R.L., Nguyen, U. & Nagler, P.L. (2015). Wide-area ratios of evapotranspiration
799 to precipitation in monsoon-dependent semiarid vegetation communities. Journal of Arid
800 Environments, 117, 84-95. https://doi.org/10.1016/j.jaridenv.2015.02.010
801 Guo, G.D., & Wu, T.H. (2007). Responses of permafrost to climate change and their environmental
802 significance, Qinghai-Tibet Plateau, J. Geophys. Res, 112, F02S03. https://doi.org/10.1029/2006J
803 F000631.
804 Gascoyne, M., Wuschke, D.M., & Durrance, E.M. (1993). Fracture detection and groundwater flow
805 characterization using He and Rn in soil gases, Manitoba, Canada. Applied Geochemistry, 8, 223-
806 233. https://doi.org/10.1016/0883-2927(93)90037-H
807 Ge, S.M., Wu, Q.B., Lu, N., Jiang, G.L., & Ball, Li. (2008). Groundwater in the Tibet Plateau,
808 western China. Geophysical Research Letters, 35(18), 80-86. https://doi.org/10.1029/2008GL03
809 4809
810 Gao, Y.H., Xia, L., Leung, L.R., Chen, D.L., & Xu, J.W. (2015). Aridity changes in the Tibetan
811 Plateau in a warming climate. Environ. Res. Lett, 10(3), 034013. https://doi.org/10.1088/1748-
812 9326/10/3/034013.
813 Hartmut, W., Hafzullah, A., Konrad, & Miegel. (2019). Fast response of groundwater to heavy
814 rainfall. Journal of Hydrology, 571, 837–842. https://doi.org/10.1016/j.jhydrol.2019.02.037
815 Ingebritsen, S.E., & Manning, C.E. (1999). Geological implications of a permeability-depth curve
816 for the continental crust. Geology, 27, 1107–1110.https://doi.org/10.1130/0091-7613(1999)0272.3.
817 CO;2
818 Ji, Z., & Kang, S., (2013). Double-nested dynamical downscaling experiments over the Tibetan
819 Plateau and their projection of climate change under two RCP scenarios. Journal of the Atmospheric
820 Sciences, 70(4), 1278–1290. https://doi.org/10.1175/JAS-D-12-0155.1
821 Kendall, C., & McDonnell, J. J. (1998). Isotope Tracers in Catchment Hydrology. Elsevier.

https://doi.org/10.1029/99EO00193

Jasechko, S., Perrone, D., Befus, K.M., Cardenas, M.B., Ferguson, G., Gleeson, T., et al. (2017). Global aquifers dominated by fossil groundwaters but wells vulnerable to modern contamination. Nature Geoscience, 10, 425–429. https://doi.org/doi:10.1038/ngeo2943

Jiang, W. J., Wang, G. C., Sheng, Y, Z., Shi, Z. M., & Zhang, H. (2019). Isotopes in groundwater (^{2}H, ^{18}O, ^{14}C) revealed the climate and groundwater recharge in the Northern China. Science of the Total Environment, 666, 298–307. https://doi.org/10.1016/j.scitotenv.2019.02.245

Jiao, J. J., Zhang, X., Liu, Y., & Kuang, X. (2015). Increased Water Storage in the Qaidam Basin, the North Tibet Plateau from GRACE Gravity Data. PLoS One, 10(10), e0141442. https://doi.org/10.1371.

Krishnaswami, S., Graustein, W. C., Turekian, K. K., & Dowd, J. F. (1982). Radium, thorium and radioactive lead isotopes in groundwaters: application to the in situ determination of adsorption-desorption rate constants and retardation factors. Water Resources Research, 6, 1663-1675.

Kuang, X., & Jiao, J. J. (2016). Review on climate change on the Tibetan Plateau during the last half century. Journal of Geophysical Research Atmospheres, 121(8), 3979-4007. https://doi.org/10.1029/WR018i006p01663

Kennedy, B. M., Lynch, M. A., & Smith, S. P. (1985). Intensive sampling of noble gases in fluids at Yellowstone. I. Early overview of the data; regional patterns. Geochimica et Cosmochimica Acta, 49, 1251–1261. https://doi.org/10.1016/0016-7037(85)90014-6

Kennedy, B. M., & Matthijs, C.S. (2006). A helium isotope perspective on the Dixie Valley, Nevada, hydrothermal system. Geothermics, 35(1), 26-43. https://doi.org/10.1016/j.geothermics.2005.09.004

Kreutz, K. J., Wake, C. P., Aizen, V. B., Cecil, L. D., & Synal, H. A. (2003). Seasonal deuterium excess in a TienShan icecore: influence of moisture transport and recycling in Central Asia. Geophysical Research Letters, 30 (8). https://doi.org/10.1029/2003GL017896

Kong, Y. L., Wang, K., Pu, T., & Shi, X. (2019). Non-monsoon precipitation dominates groundwater recharge beneath a monsoon affected glcacier in Tibetan Plateau. Jounral of Geophisical Research: Atmospheres, 124(10), 10913-10930. https://doi.org/10.3390/w11061239

Klinger, Y., Xu, X. W., Tapponnier, P., Van, W. J., Lasserre, C., & King, G. (2005). High resolution satellite imagery mapping of the surface rupture and slip distribution of the Mw 7.8, 14 November 2001 Kokoxili Earthquake, Kunlun Fault, Northern Tibet. Bulletin of the Seismological Society of

America, 95(5), 1970–1987. https://doi.org/10.1785 / 0120040233

Li, Z. X., Li Z. J., Feng, Qi., Zhang, B. J., Gui, J., Xue, J., & Gao, W. D. (2020). Runoff dominated by supra-permafrost water in the source region of the Yangtze river using environmental isotopes. Journal of Hydrology, 582. 125-140. https://doi.org/10.1016/j.jhydrol.2019.124506

Ma, J. Z., Ding, Z. Y., Edmunds, W. M., Gates J. B., & Huang, T. M. (2009). Limits to recharge of groundwater from Tibetan plateau to the Gobi desert, implications for water management in the mountain front. Journal of Hydrology, 364, 128–141. https://doi.org/10.1016/j.jhydrol.2008.10.010

Malard, A., Sinreich, M., & Jeannin, P. Y. (2016). Anovel approach for estimating karst groundwater recharge in mountainous regions and its application in Switzerland. Hydrological Processes, 30(13), 2153–2166. https://doi.org/10.1002/hyp.10765

Mark, D. (2003). Mountain and subpolar glaciers show an increase in sensitivity to climate warming and intensification of the water cycle. Journal of Hydrology, 282(1–4), 164-176. https://doi.org/ 10.1016/S0022-1694(03)00254-3

Morgenstern, U., Stewart, M.K., & Stenger, R. (2010). Dating of stream water using tritium in a post nuclear bomb pulse world: continuous variation of mean transit time with streamflow. Hydrology and Earth System Sciences, 14, 2289–2301. https://doi.org/10.5194/hessd-7-4731-2010

Pradeep, K. A., Joel, R. G., & Klaus, F. F. (2005). Isotopes in the water cycle: past, present and future of a developing science. Springer Netherlands. https://doi.org/10.1007/1-4020-3023-1

Post, V.E.A., Groen, J., Kooi, H., Person, M., Ge, S., & Edmunds, W. M. (2013). Offshore fresh groundwater reserves as a global phenomenon. Nature, 504, 71–78. https://doi.org/10.1002/hyp. 10765

Phillips, F.M., Mills, S., Hendrickx, M.H., & Hogan, J. (2003). Environmental tracers applied to quantifying causes of salinity in arid-region rivers: results from the Rio Grande Basin, Southwestern USA. Elsevier, Developments in water science, 50, 327-334. https://doi.org/10.1016/S0167-5648(03)80029-1

Rangwala, I., Miller, J. R., Russell, G. L., & Xu, M. (2010). Using a global climate model to evaluate the influences of water vapor, snow cover and atmospheric aerosol on warming in the Tibetan Plateau during the twenty-first century. Climate Dynamics, 34(6), 859–872, https://doi.org/10.1007/ s00382-009-0564-1

Sun, C. Y. (1991). Isotope hydrogeology in Golmud area. Qinghai Geology, 1, 26-31. https://doi.org/ CNKI:SUN:GTJL.0.1991-01-003

884 Salamon, T. (2016). Subglacial conditions and Scandinavian Ice Sheet dynamics at the coarse-
885 grained substratum of the fore-mountain area of southern Poland. Quaternary Science Reviews, 151,
886 72–87. https://doi.org/10.1016/j.quascirev.2016.09.002
887 Sergey, A. S., & Vladimir, N. G. (2009). Snow isotopic content change by sublimation. Journal of
888 Glaciology, 55(193), 823-829. https://doi.org/10.3189/002214309790152456
889 Smerdon, B.D. (2017). Groundwater recharge: The intersection between humanity and
890 Hydrogeology. Journal of Hydrology, 555, 909–911. https://doi.org/10.1016/j.jhydrol.2017.10.075
891 Smerdon, B.D., Gardner, W. P., Harrington, G. A., & Tickell, S. J. (2012). Identifying the
892 contribution of regional groundwater to the baseflow of a tropical river (Daly River, Australia).
893 Journal of Hydrology, 464, 107–115. https://doi.org/10.1016/j.jhydrol.2012.06.058
894 Sun, Q. H., Miao, C. Y., & Duan Q.Y. (2015). Projected changes in temperature and precipitation in
895 ten river basins over China in 21st century. International journal of climatology, 35(6), 1125–1141.
896 https://doi.org/10.1002/joc.4043
897 Su, X., Xu, W., Yang, F., & Zhu, P. (2015). Using new mass balance methods to estimate gross
898 surface water and groundwater exchange with naturally occurring tracer 222Rn in data poor regions:
899 a case study in northwest China. Hydrological Processes, 29(6), 979–990. https://doi.org/10.1002/
900 hyp.10208
901 Tan, H. B., Chen, J., Rao, W. B., Zhang, W. J., & Zhou, H. F. (2012). Geothermal constraints on
902 enrichment of boron and lithium in salt lakes: an example from a river-salt lake system on the
903 northern slope of the eastern Kunlun mountains, China. Journal of Asian Earth Sciences, 51, 21-29.
904 https://doi.org/10.1016/j.jseaes.2012.03.002
905 Tolstinkhin, I., Lehmann, B. E., & Loosli, H. H. (1996). Helium and argon isotopes in rocks,
906 minerals, and related groundwaters: A case study in northern Switzerland. Geochimica et
907 Cosmochimica Acta, 60, 1497–1514. https://doi.org/10.1016/0016-7037(96)00036-1
908 Tan, H. B., Rao, W. B., Chen, J. S., Su, Z. G., Sun, X. X., & Liu, X. Y. (2009). Chemical and isotopic
909 approach to groundwater cycle in western Qaidam Basin, China. Chinese Geographical Science,
910 19(4), 357-364. https://doi.org/CNKI:SUN:ZDKX.0.2009-04-010
911 Tian, L. D., Yao, T.D., MacClune, K., White, J. W. C., Schilla, A., Vaughn, B., et al. (2007). Stable
912 isotopic variations in west China: a consideration of moisture sources. Journal of Geophysical
913 Research, 112 (D10). https://doi.org/10.1029/2006JD007718
914 Weiss, R. F. (1971). Solubility of Helium and neon in water and sea water. Jour. Chem. Eng. Data,

16, 235–241. https://doi.org/10.1021/je60049a019

Wang, Y.G., Guo, H.Y., Li, J., Huang, Y., Liu, Z.Y., Liu, C.E., et al. (2008). Investigation and Assessment of Grounderwater Resources and Their Environmental Issues in the Qaidam Basin. Geological Publishing House, 23-28.

Wang, Y., Wei, J. H., & Xie, H. W. (2018). The variation of terrestrial water storage in the Qaidam Basin based on GRACE data. South-to-North Water Transfers and Water Science & Technology, 01. https://doi.org/10.13476/j.cnki.nsbdqk.20180012

Wang, X., Yang, M., Liang, X., Pang, G., Wan, G., Chen, X., & Luo, X. (2014). The dramatic climate warming in the Qaidam Basin, northeastern Tibetan Plateau, during 1961–2010. International journal of climatology, 34(5), 1524–1537. https://doi.org/10.1002/joc.3781

Wang, Y. D., Zheng, J. J., Zhang, W. L., Li S.Y., Liu, X.W., Yang, X., & Liu, Y. H. (2012). Cenozoic uplift of the Tibetan Plateau: Evidence from the tectonice-sedimentary evolution of the western Qaidam Basin. Geoscience Frontiers, 3(2), 175-187. https://doi.org/10.1016/j.gsf.2011.11.005

Xiao, Y., Shao, J.L., Cui, Y.L., Zhang, G., & Zhang, Q.L. (2017). Groundwater circulation and hydrogeochemical evolution in Nomhon of Qaidam Basin, northwest China. Journal of Earth System Science, 126 (2), UNSP 26. https://doi.org/10.1007/s12040-017-0800-8

Xu, W., Su, X.S., Dai, Z.X., Yang, F.T., Zhu, P.C., Huang, Y. (2017). Multi-tracer investigation of river and groundwater interactions: a case study in Nalenggele River basin, northwest China. Hydrogeology Journal 25(7), 2015-2029. https://doi.org/ 10.1007/s10040-017-1606-0

Xiao, Y., Shao, J.L., Frape, S.K., Cui, Y.L., Dang, X.Y., Wang, S.B., & Ji, Y.H. (2017). Groundwater origin, flow regime and geochemical evolution in arid endorheic watersheds: a case study from the Qaidam Basin, northwest China. Hydrology and Earth System Sciences, 4381-4400. https://doi. org/ 10.5194/hess-2017-647.

Xiang, L., Wang, H., Steffen, H., Wu, P., Jia, L., Jiang, L., & Shen, Q. (2016). Groundwater storage changes in the Tibetan Plateau and adjacent areas revealed from GRACE satellite gravity data. Earth and Planetary Science Letters, 449, 228–239. https://doi.org/10.1016/j.epsl.2016.06.002

Yang, J.P., Ding, Y.J., & Chen, R.S. (2007). Climatic causes of ecological and environmental variations in the source regions of the Yangtze and Yellow rivers of China. Environ. Geol, 53, 113–121. https://doi.org/ 10.1007/s00254-006-0623-4

You, Q.L., Min, J.Z., & Kang, S.C. (2015). Rapid warming in the Tibetan Plateau from observations and CMIP5 models in recent decades. Int. J. Climatol., https://doi.org/10.1002/joc.4520

Yin, G.H., Shen, J., & Jiang, J.X. (2002). Tectonic background of the Ms 8.1 earthquake on 14 Nov, 2001 at east Kunlun fault. Arid Land Geography, 25(1), 24-29. https://doi.org/10.3969/j.issn.1001-8956.2002.01.001

Ye, X.R., Tao, M.X., Yu, C.A., & Zhang, M.J. (2007). Helium and neon isotopic compositions in the ophiolites from the Yarlung Zangbo River, Southwestern China: The information from deep mantle. Science in China (Ser. D), 50 (6): 801–812. https://doi.org/10.1-007/s11430-007-0017-9

Yael, K., Yishai, W., Abraham, S., & Yoseph, Y. (2015). Application of radon and radium isotopes to groundwater flow dynamics: An example from the Dead Sea. Chemical Geology, 411, 155–171. https://doi.org/ 10.1016/j.chemgeo.2015.06.014

Zhou, H., Chen, L., Diwu, C.R., & Lei, C. (2018). Cenozoic uplift of the Qimantage Mountains, northeastern Tibet: Contraints from provenance analysis of Cenozoic sediments in Qaidam Basin. Geological Journal, 53, 2613–2632. https://doi.org/10.1002/gj.3.095

Zhang, G.L., Dong, J.W., Zhou, C.P., Xu, X.L., Wang, M., Ouyang, H., & Xiao, X.M. (2013). Increasing cropping intensity in response to climate warming in Tibetan Plateau, China. Field Crops Research, 142 , 36–46. https://doi.org/10.1016/j.fcr.2012.11.021

Zhao, L.J., Eastoe C.J., Liu, X.H., Wang, L.X., Wang, N.L., Xie, C., & Song, Y.X. (2018). Origin and residence time of groundwater based on stable and radioactive isotopes in the Heihe River Basin, northwestern China. Journal of Hydrology: Regional Studies, 18, 31–49. https://doi.org/10.1016/j.ejrh.2018.05.002

Zhu, Y.Z., Li, W.S., Wu, B.H., & Liu, C.L. (1989). New recognition on the geology of the Yiliping Lake and the east and west Taijnar Lakes in the Qaidam Basin, Qinghai Province. Geological Review ,35 (6), 558–565. https://doi.org/10.16509/j.georeview.1989.06.009

Zhao, Z.H., Wang, D.Q., Bai, Y.L., Yan, & C.H., Xu, X.F. (2019). Research on Establishing Tritium Concentration Model of Precipitation in Northeast of Tarim Basin Based on Factor Analysis. Earth and Environmental Science, 237(2), 022014 . https://doi.org/ 10.1088/1755-1315/237/2/022014

Zhu, X.H., Wang, W.Q., & Klaus., F. (2013). Future climate in the Tibetan Plateau from a statistical regional climate model. J. Clim., 26(24), 10,125–10,138, https://doi.org/10.1175/JCLI-D-13-00187.1